

PAPER

Influence of laser pulse regime on the structure and optical properties of TiO₂ nanolayers

To cite this article: Y Peñaloza-Mendoza *et al* 2018 *Mater. Res. Express* **5** 125022

View the [article online](#) for updates and enhancements.



IOP | ebooks™

Bringing you innovative digital publishing with leading voices to create your essential collection of books in STEM research.

Start exploring the **collection** - download the first chapter of every title for free.

Materials Research Express



PAPER


Influence of laser pulse regime on the structure and optical properties of TiO₂ nanolayers

RECEIVED
31 July 2018

REVISED
29 August 2018

ACCEPTED FOR PUBLICATION
20 September 2018

PUBLISHED
28 September 2018

Y Peñaloza-Mendoza¹, F C Alvira² , F Caballero-Briones³, C Guarneros-Aguilar⁴ and L Ponce^{1,5}

¹ Instituto Politécnico Nacional, Laboratorio de Tecnología Láser, CICATA Altamira, 89600 Altamira, México

² Laboratorio de Biomembranas y Laboratorio de Instrumentación, Automatización y Control, Universidad Nacional de Quilmes, Dpto de Ciencia y Tecnología, Bernal, ZIP: 1876, Buenos Aires, Argentina

³ Instituto Politécnico Nacional, Materiales y Tecnologías para Energía, Salud y Medioambiente (GESMAT), CICATA Altamira, 89600 Altamira, México

⁴ CONACYT-Instituto Politécnico Nacional, Materiales y Tecnologías para Energía, Salud y Medioambiente (GESMAT), CICATA Altamira, 89600 Altamira, México

⁵ San Petersburg Electrotechnical University, Professora Popova 5, 197376 St. Petersburg, Russia

E-mail: fernando.alvira@unq.edu.ar

Keywords: pulsed laser deposition, multipulse and monopulse regimes, TiO₂, TiO₂ optical properties, TiO₂ structure, TiO₂ air annealing

Abstract

TiO₂ films were deposited onto glass substrates by pulsed laser deposition (PLD) in high vacuum under monopulse and multipulse excitation. After deposition, a thermal treatment on air atmosphere was done to promote crystallization. Films were studied by x-ray diffraction, energy dispersive spectroscopy, scanning electron, atomic force microscopy, UV–vis spectroscopy, and ellipsometry. After air annealing, films gain a different amount of oxygen: TiO_{1.9} in multipulse regime versus TiO_{1.7} in the monopulse one. Splashing is observed in both regimes although in the multipulse mode greater particles are found, that derived in a less compact film after annealing which could be the cause of the better oxygen diffusion. The optical band gap of the film prepared with monopulse excitation is 3.09 eV. This value increased to 3.34 eV with annealing, corresponding to that of anatase. The film made with multipulses has an $E_g = 3.12$ eV which was invariant upon annealing. The difference in the properties of the films grown in the different regimes was attributed to the re-excitation of the plasma during the ablation process in the multipulse ablation that leads to an increased splashing density and thereafter a less compact film and the presence of off-stoichiometry inclusions within the film bulk.

1. Introduction

Pulsed laser deposition (PLD) technique is a widely known deposition technique whose operating principle relies on the removal of material by laser ablation from a surface [1]. The plasma formed during the ablation process expands at high speeds (approximately 400 ms^{−1}) with a well-defined direction and finally condenses on a substrate to form the thin film [2]. One of the exciting particularities of PLD is that the target stoichiometry is usually kept intact in contrast, for example, with RF sputtering [3]. Opposite to the simplicity of the operation, the phenomena involved in PLD are very complicated. One of the primary disadvantages of this technique is the ejection of fused material during the ablation process via a phenomenon known as splashing, which can be observed in the form of micrometric and sub-micrometric droplets on the surface of the generated film [4–6]. Most of the studies have reported thin films fabricated using PLD in single-pulse emission regime. In the literature, there are some papers dealing with laser ablation under multipulse excitation, those studies have shown that the splashing effect can be significantly reduced/eliminated using a second laser parallel or collinear to the target that re-excites the plasma where each laser emission was composed of multiple pulses with an interpulse separation between 10 and 100 μs [7, 8]. In a recent study, some of the interactions reported by Galbacs *et al* were confirmed using the multi-pulse regime to deposit titanium dioxide (TiO₂) thin films, demonstrating that a lower deposition rate and roughness is obtained when using the multi-pulse regime for the same total emission energy, attributable to enhanced adatom mobility after plasma reexcitation [8, 9].

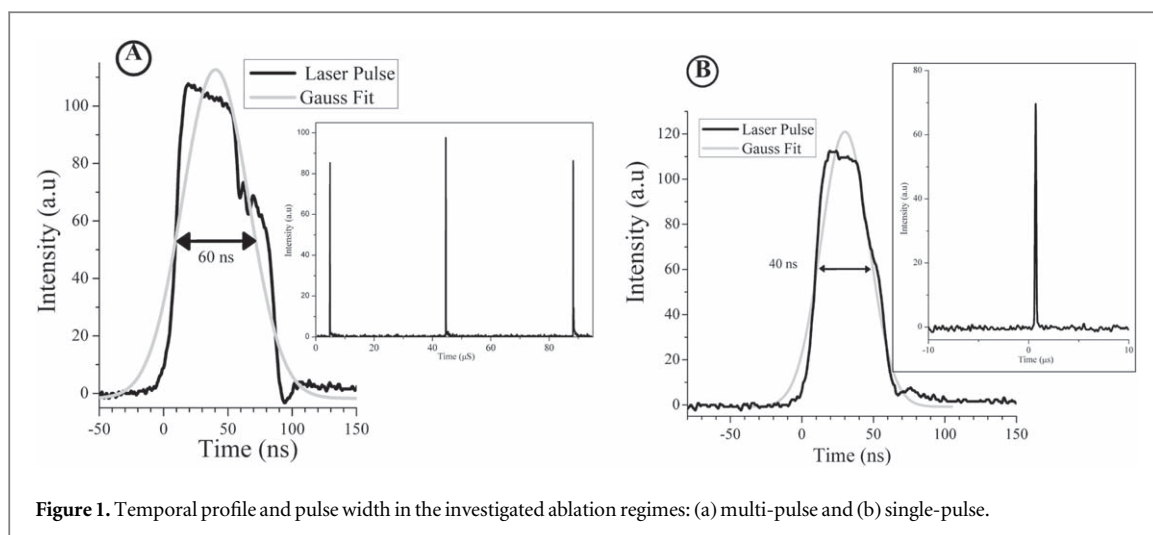


Figure 1. Temporal profile and pulse width in the investigated ablation regimes: (a) multi-pulse and (b) single-pulse.

TiO₂ is an n-type semiconductor that has emerged as an extremely valuable oxide for numerous applications because of its unique electrical and optical characteristics, in addition to being non-toxic and inexpensive [10]. TiO₂ in thin film form has a large variety of applications in photocatalysis, photovoltaic and optical systems such as in multilayer structures that can be anti-reflective or exhibit high reflectivity at a specific wavelength [11–13]. The most significant limitation for TiO₂ use in photocatalysis and photovoltaics is its low absorption in the visible region. Thus there are substantial efforts in sensitizing TiO₂ with visible absorbing materials or by producing non-stoichiometric TiO₂, i.e., TiO_{2-x} which is usually known as ‘black’ TiO₂ [14, 15]. On the other hand, in photocatalysis and photovoltaic applications anatase is the phase of choice because of its higher photoelectron yield, while rutile is most used in optical devices because of its higher stability [16, 17].

This paper aims to compare the structure, composition, morphology and optical properties of TiO₂ films with similar thickness, as-grown and after an air annealing, deposited with multi and monopulse laser excitation under high vacuum.

2. Methods

The films were deposited by PLD on soda-lime glass substrates using a commercial TiO₂ target (Kurt J Lesker with a purity of 99.99%). In the ablation process, a Nd:YAG laser with a passive Cr⁴⁺:YAG Q-Switch was employed; the laser emitted at 1064 nm and was operated at a frequency of 10 Hz. The deposition was performed at 5×10^{-5} Torr, with a target-substrate distance of 5 cm and a substrate temperature of 130 °C. The laser system was configured to emit in the single-pulse and multi-pulse regimes. In the initial configuration, the laser module emitted in the multi-pulse regime, where each emission comprised three individual pulses with a duration of 60 ns separated each one by 45 μ s (see figure 1(a)). In the second configuration, an additional Cr⁴⁺:YAG Q-Switch was added to the optical cavity of the laser, reducing the emission to a single pulse of 40 ns (see figure 1(b)).

The total energy for each emission was adjusted to 104 mJ in both regimes, which fixed the working fluence at 2 J.cm^{-2} . In this paper ‘mono pulse’, ‘single pulse’ or ‘single laser pulse’ means a burst of pulses, i.e., a laser shot, composed by only one laser pulse, similarly ‘multipulse’ or ‘multipulse laser’ means a burst of 3 individual pulses. In other words, when we mention ‘sample prepared by 6000 pulses impinging the target’, if the regimen was single pulse, it means that 6000 individual pulses impinged the target. Otherwise, when we refer to 12 000 pulses in multipulse regime, it means that 36 000 ($12\,000 \times 3$) laser pulses did impinge the sample.

In a previous contribution, the relation of the number of shots against the film thickness was studied [9]. It was found that multipulse regime leads to reduced growth rate and lower surface roughness, thus, in the present contribution a comparative study was conducted by growing films with similar thicknesses of ca. 64 nm in both regimes, i.e., the films were obtained using 6000 laser shots for the single-pulse regime and 12 000 laser shots for the multi-pulse regime respectively. The analysis consisted of evaluating the morphology by scanning electron microscopy (SEM) and atomic force microscopy (TT AFM Workshop) with a Si tip in the contact mode. The optical properties were evaluated by UV–vis–NIR spectroscopy (Cary 5000, Agilent Technologies) and spectroscopic ellipsometry (Uvisel LT M200AGMS, HORIBA Jobin Yvon). The chemical composition of the films was determined by energy dispersive x-ray spectroscopy (EDS) (Apollo XL-SDD, EDAX) and the crystalline structure by x-ray diffraction (XRD) using the grazing incidence configuration with the incident beam at 1.5° (X Pert PRO MRD, PANalytical). Films were characterized before and after a post-deposition

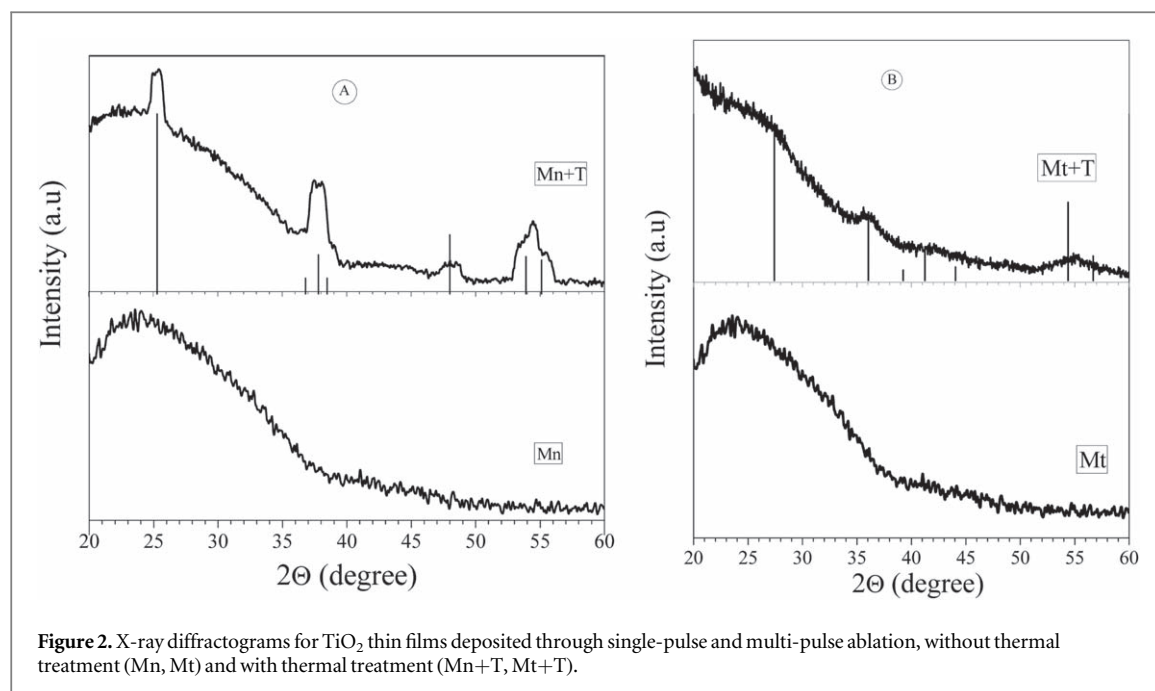


Figure 2. X-ray diffractograms for TiO_2 thin films deposited through single-pulse and multi-pulse ablation, without thermal treatment (Mn, Mt) and with thermal treatment (Mn+T, Mt+T).

Table 1. Film nomenclature.

Label	Sample
Mn	Thin film made by single-pulses
Mn+T	Thin film made by single-pulses with thermal treatment
Mt	Thin film made by multi-pulses
Mt+T	Thin film made by multi-pulses with thermal treatment

thermal treatment done in the air for 2 h at 500 °C. Table 1 shows the nomenclature used to refer to the investigated samples.

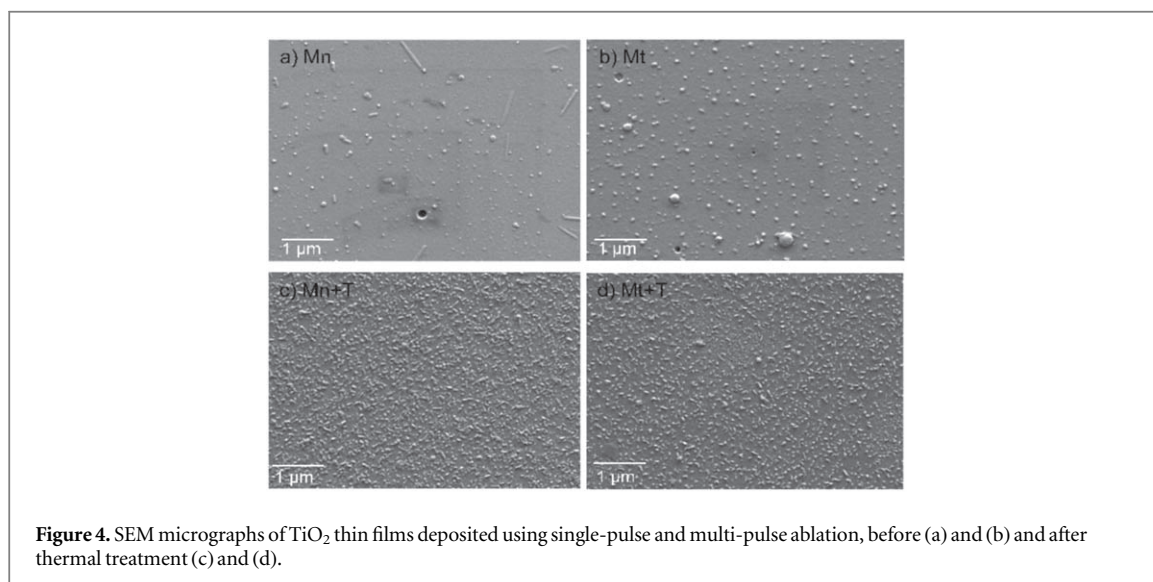
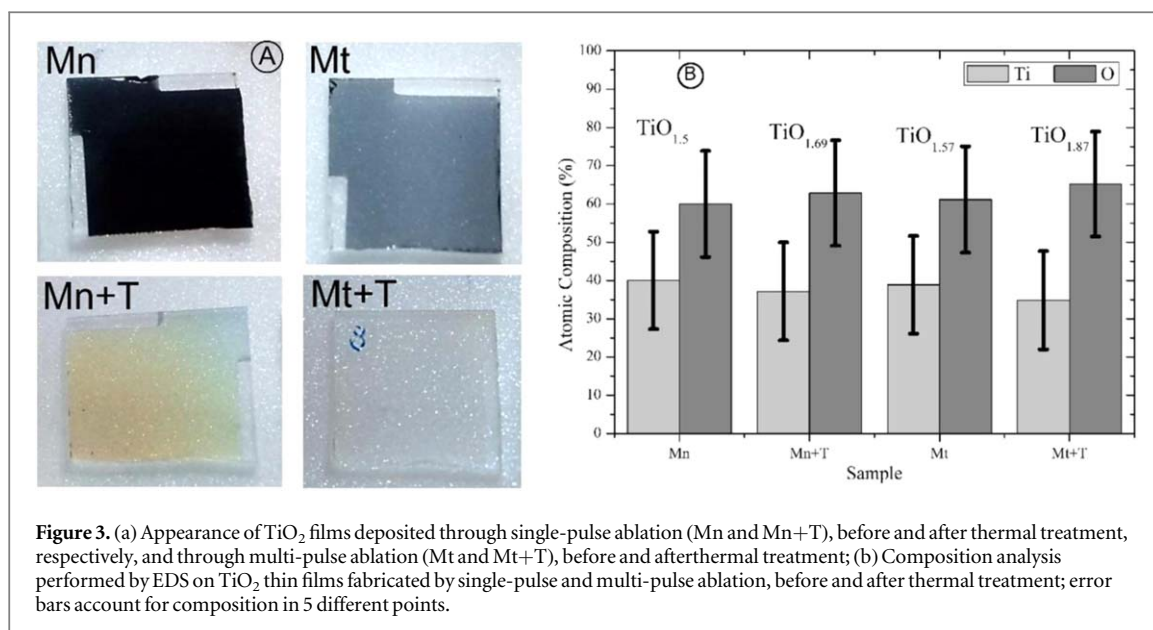
3. Results and discussions

3.1. Crystalline structure

Figure 2 shows the XRD diffractograms obtained for the samples with and without thermal treatment. Before thermal treatment, no diffraction peaks are observed indicating that the films are amorphous for both ablation regimes. The film grown in the single-pulse regime shows diffraction peaks corresponding to the anatase phase after thermal treatment is done. By another way, the multi-pulse-deposited film exhibits diffraction peaks corresponding to the rutile phase. The observed peaks are broad and have a low intensity, indicating that there is an early or partial transition to the crystalline phase. Sharma *et al* suggested that the grains and voids in the films may form differently depending on the plasma energy and laser wavelength used for ablation [18]. In that reference, films produced from more energetic plasma generated at 355 nm and thermal treatment at 600 °C resulted in the formation of the rutile-brookite phase. By another way at 1064 nm with less energetic plasma, the same thermal treatment induced a transition to the anatase-brookite phase. Following our previously published analyses, it is possible to assume that the plasma was re-excited in the multi-pulse regime in the ablation process, i.e., this plasma is more energetic than that generated in the single-pulse regime, thus creating adatoms with higher energy, this could be a plausible explanation of the transition to the rutile phase with thermal treatment in the sample grown using multi-pulses [9, 19].

3.2. Composition

Figure 3 presents the photographs of the samples prepared before and after thermal treatment. The color of the untreated films varies from black to light blue, suggesting that these films would contain either amorphous semi-metallic Ti–O entities or Ti suboxide inclusions as due to oxygen deficiency. After thermal treatment, both samples exhibit lighter tones, which are indicative of oxygen incorporation and film crystallization, as observed in the XRD results.



The oxygen and titanium content in the films was quantified using EDS and presented in figure 3(b) together with the estimated ‘compounds’ formulae. The films deposited using multi-pulses have a higher O/Ti ratio before thermal treatment, with a composition of TiO_{1.6}, whereas the films formed in the single-pulse regime have a structure of TiO_{1.5}. The thermal treatment increased the O/Ti ratio in both samples; however, the film deposited with multi-pulses after thermal treatment follows most closely the TiO₂ stoichiometry, with an O/Ti ratio of 1.9. Meng *et al* attributed oxygen losses in films growth by sputtering, to the low friction coefficient of these deposits relative to that of Ti [3]. Considering Meng’s hypothesis, oxygen is more volatile than Ti and is, therefore, more vulnerable to the deviation of the propagation trajectory of the plasma plume during the growth process, which would reduce the O/Ti ratio in both films. However, the difference between the O/Ti ratios in the two regimes remains as a subject for future research. A remarkable result is the possibility to obtain ‘black-TiO₂’ by PLD; in a future work a more extensive study on the films properties prepared without air annealing, for example in photocatalysis applications, is intended.

Figures 4(A) and (B) show the SEM micrographs for the films deposited in the single-pulse and multi-pulse regimes, respectively, as reported in [9]. The splashing effect produced the large particles in the images for both regimes. However, the films grew using multi-pulses exhibit droplet-shaped particles, whereas the particles in the film grown using single-pulses have a peculiar, elongated form and a lower particle density. Figures 4(C) and (D) show the micrographs of the films after thermal treatment. The film surface is restructured in both deposits, and the particles produced by splashing are no longer observed. Instead, there are many irregularly shaped particles, suggesting that a re-nucleation process occurred at the material surface, because of the

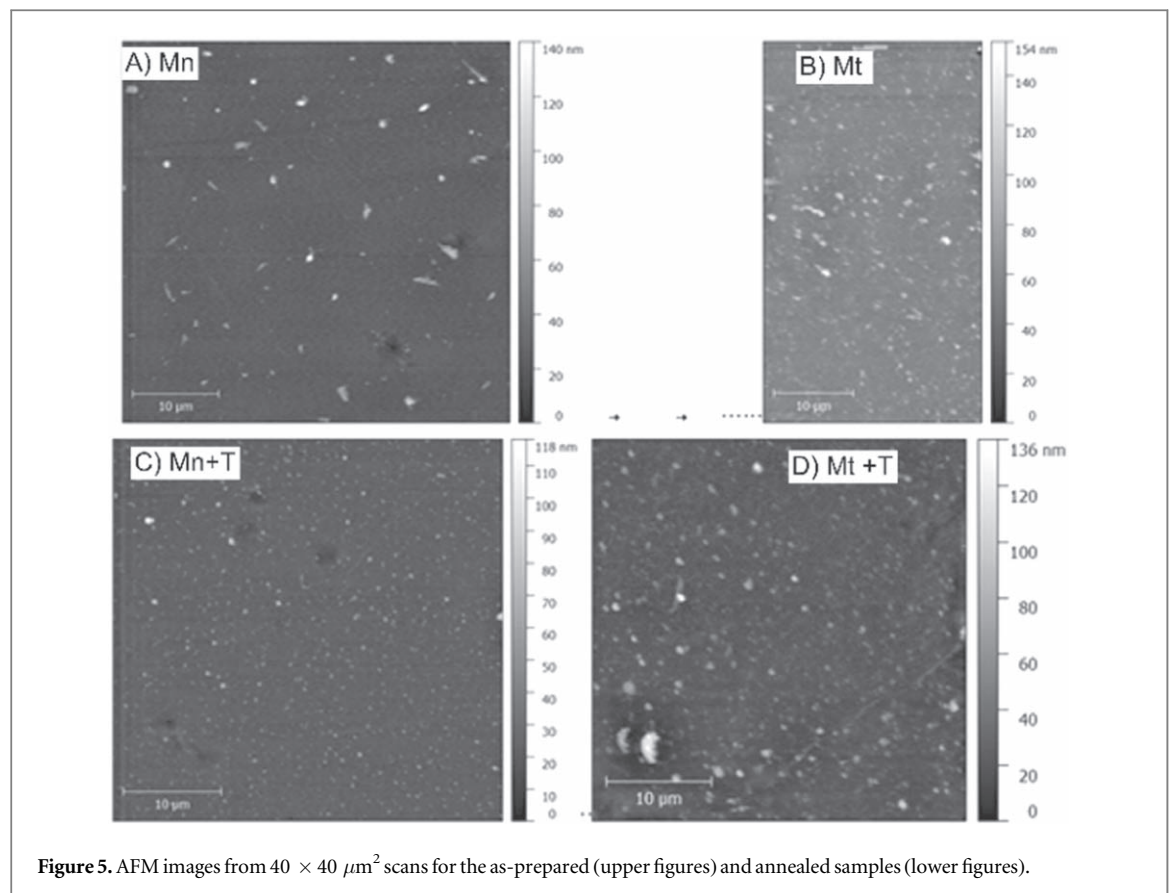


Figure 5. AFM images from $40 \times 40 \mu\text{m}^2$ scans for the as-prepared (upper figures) and annealed samples (lower figures).

formation of a crystalline phase as observed in XRD. The surface of the annealed film prepared with multipulse excitation seems less compact for that of the annealed sample prepared in the monopulse regime, in correspondence to the AFM data in which indicate that R_{rms} roughness is slightly higher within the number of laser shots used for the deposition of these particular films [9].

Figure 5 shows the AFM images from $40 \times 40 \mu\text{m}^2$ scans for both deposition cases, before and after thermal treatment. Figures 5(A) and (B) present the pictures of the as-deposited films; the film prepared with monopulse excitation presents elongated structures, and droplets sparsely spread all over the surface in comparison with the surface of the film made with multipulse excitation where more droplets are observed although non-elongated structures appear.

After film annealing, the surface of the film prepared with single pulses seems more compact, with smaller dots while the image of the film made with multipulses still presents a surface decorated with dots of similar appearance upon annealing, the particle sizes decrease in the films deposited with single pulses; on the other hand, the particles are around the same size no matter the annealing for the case of the films deposited with multipulses.

Figures 6(A) and (B) display three representative linear profiles for each sample, obtained from the AFM images, to represent the particles observed in the surface. It can be readily seen that.

Figure 6(C) presents the height distribution obtained from the AFM $40 \times 40 \mu\text{m}^2$ images for both deposition cases, before and after thermal treatment with the R_{rms} values indicated. All the distributions are symmetric, suggesting that a single nucleation event followed by nuclei growth on subsequent shots is the predominant mechanism. The height distribution of the film deposited by single-pulses (Mn) shows a mean height of 27 nm and roughness of 7 nm; upon annealing (Mn+T) the average height reduces to 21 nm and the roughness to 5 nm. Correspondingly, the film as-deposited using multi-pulses (Mt) exhibits an average height of 61 nm with a R_{rms} of 8 nm that reduce upon annealing (Mt+T) to 27 nm with a slight increment in R_{rms} to 9 nm. For the particle size distribution, the films prepared with single pulses are narrower than those prepared with multipulses. Annealing tends to reduce the distribution width. The observed trends in the AFM morphology and surface roughness coincide with those seen in the SEM images and can be attributed to recrystallization and strain relaxation upon annealing [20]. The large particle size in the as-deposited film Mt (multipulses) is consistent with a significant amount of splashed particles.

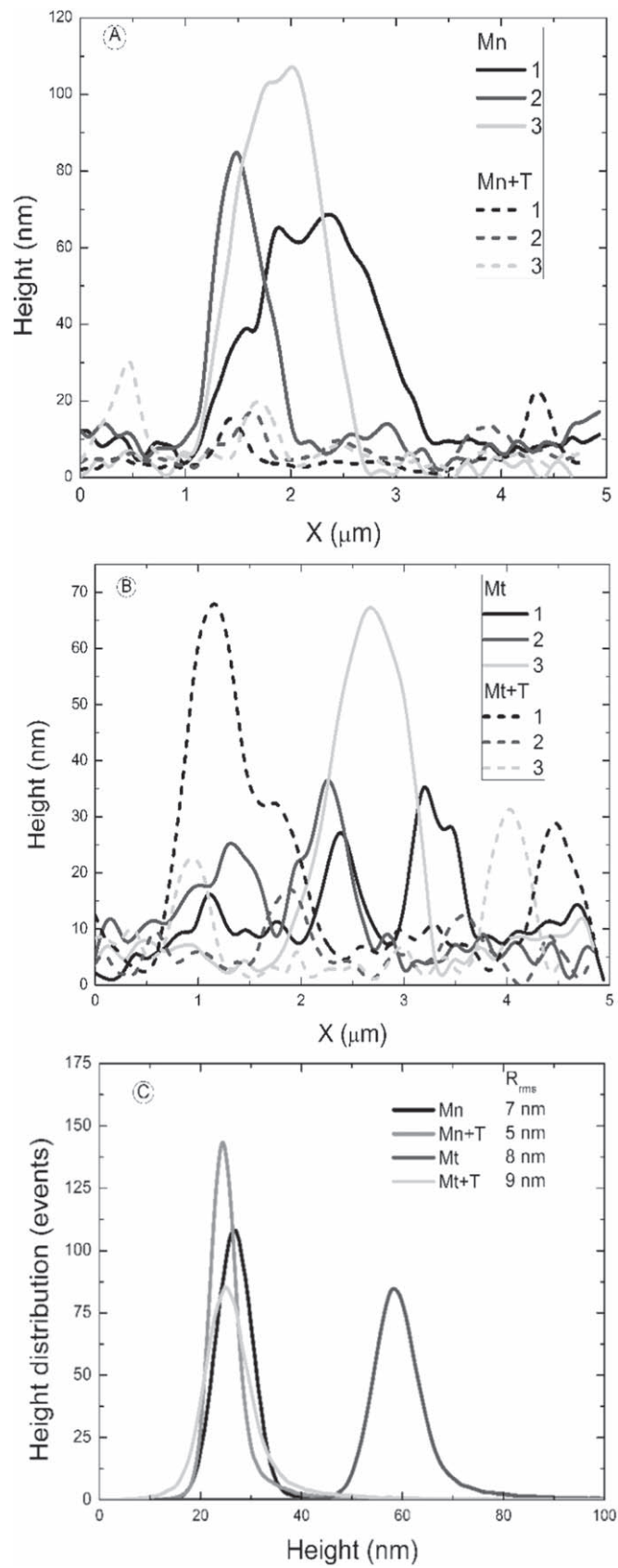
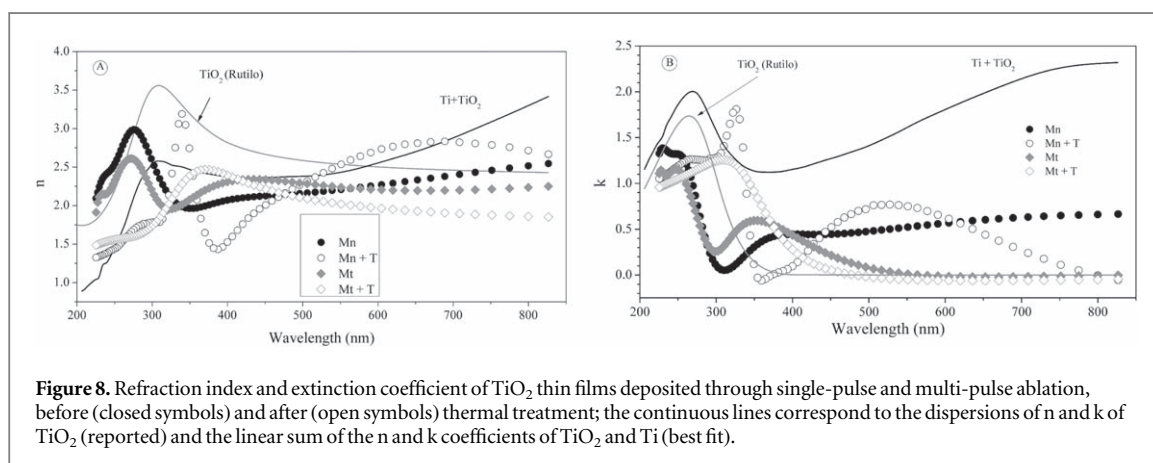
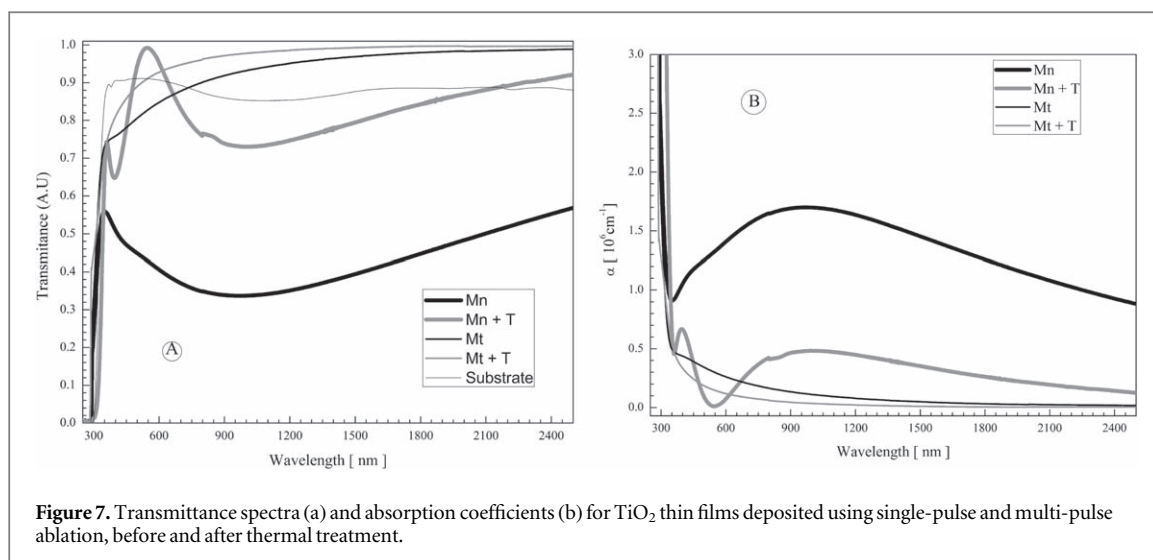


Figure 6. Linear profiles obtained from the AFM images for the sample prepared with single pulses (figure (A)) and multipulses (figure (B)), before and after annealing. Height distribution for TiO₂ thin films fabricated with single-pulse and multi-pulse ablation (figure (C)), before and after thermal treatment.



3.3. Optical properties

Figure 7 shows the transmittance spectra of the films prepared in both regimes, with and without thermal treatment, compared to that of the glass substrate as well as the absorption coefficients of the films (α) as a function of the wavelength. There is a very sharp difference in the spectra between the two regimes, with the film prepared using multi-pulses exhibiting a transmittance above 0.9 in the medium range and starting to absorb strongly at approximately 350 nm, which corresponded to the TiO₂ absorption [21]. The spectrum for the film grown using single-pulses exhibits a maximum absorption centered at approximately 900 nm and after annealing, another absorption peak near 450 nm. The maximum absorption at 900 nm and 450 nm could be attributed to the insufficient incorporation of oxygen during film growth and the possible formation of Ti suboxides, which would be consistent with the dark coloration of the film. The absorption spectra of the films prepared with multipulses display a monotonous behavior, i.e., no absorption peaks before the edge at ca. 350 nm and only a short absorption tail that reduces upon annealing.

Figure 8 shows the refractive index (n) and the extinction coefficients (k) dispersion of the films for the wavelength, obtained by spectroscopic ellipsometry at a 70° angle. The n values of all the samples are within the reported range for TiO₂ (2.3–2.7). The n and k dispersions of the film deposited using ablation with multi-pulses and without thermal treatment coincide with those reported by Cronmeyer *et al* for amorphous TiO₂. The spectrum for the film grown using single-pulses exhibits a maximum absorption centered at approximately 900 nm and after annealing, another absorption peak near 450 nm. The maximum absorption at 900 nm and 450 nm could be attributed to the insufficient incorporation of oxygen during film growth and the possible formation of Ti suboxides, which would be consistent with the dark coloration of the film. The absorption spectra of the films prepared with multipulses display a monotonous behavior, i.e., no absorption peaks before the edge at ca. 350 nm and only a short absorption tail that reduces upon annealing.

Figure 8 shows the refractive index (n) and the extinction coefficients (k) dispersion of the films for the wavelength, obtained by spectroscopic ellipsometry at a 70° angle. The n values of all the samples are within the reported range for TiO₂ (2.3–2.7). The n and k dispersions of the film deposited using ablation with multi-pulses

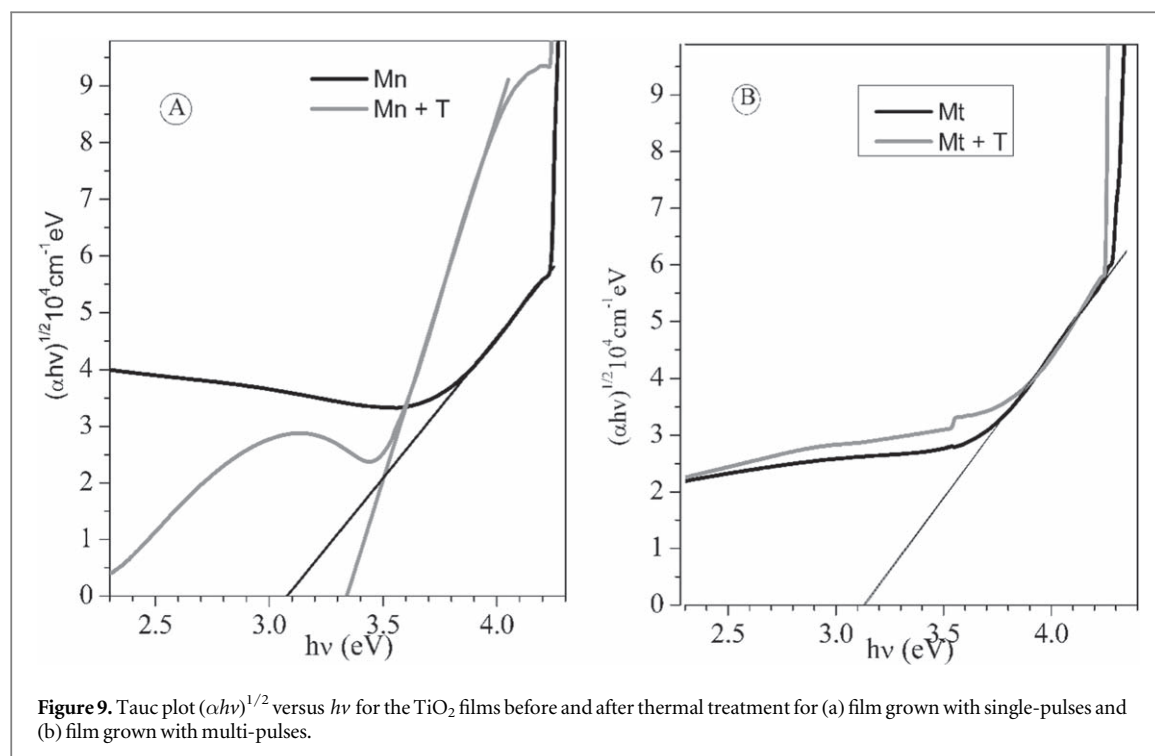


Figure 9. Tauc plot $(\alpha h\nu)^{1/2}$ versus $h\nu$ for the TiO_2 films before and after thermal treatment for (a) film grown with single-pulses and (b) film grown with multi-pulses.

and without thermal treatment coincide with those reported by Cronmeyer *et al* for amorphous TiO_2 [22]. However, neither of the dispersions coincides with the stable phases of TiO_2 , rutile, anatase or brookite. Both dispersions tend to increase toward the infrared range, particularly for the sample prepared using single-pulses. The n and k dispersions were compared with a simulated spectrum consisting of a linear sum of the indexes n and k that have been reported for TiO_2 and Ti. From the observed behavior, it can be concluded that the dispersions reflect the presence of non-stoichiometric Ti-oxide inclusions.

The samples grown with single pulses and subjected to thermal treatment exhibits a refraction index that decreased sharply in the region between 350 and 400 nm following a considerable increase in the visible region and then gradually decreases approximately in the infrared region. This erratic behavior may result from the formation of suboxides. The extinction coefficient decreases rapidly very near 370 nm, which corresponded to an absorption edge very close to that of anatase (383 nm) [23]. However, the dispersion in the visible region indicates a strong absorption that does not correspond to that crystalline phase.

For the sample deposited using multi-pulses, thermal treatment decreases the n value in the visible-infrared region, maintaining the dispersion characteristics of TiO_2 , whereas k was approximately zero, confirming that stoichiometric TiO_2 formation caused the reduction in the absorption in the region mentioned above.

Figure 9 shows Tauc graphs for an indirect transition of TiO_2 for calculation of the forbidden band gap (E_g) in the films deposited with both laser regimes, before and after thermal treatment [24]. For the film grown using multi-pulses the calculated band gap is 3.12 eV, within the range of the reported values for rutile, and did not change after thermal treatment [18]. However, the thermal treatment shifts the band gap of the film formed with single-pulse deposition from 3.09 eV to 3.34 eV. The latter value was within the range of the calculated values for anatase of 3.23–3.59 eV, which indicates that the anatase phase may have nucleated [18]. The results are consistent with the XRD diffractograms of the studied samples.

4. Conclusions

High vacuum pulsed laser deposition deposited TiO_2 films under monopulse and multipulse excitation. The structure, composition, morphology and optical properties were studied to compare the effects of the laser pulse regime as well as that of an air annealing. As-deposited films are amorphous although, upon annealing, the film prepared with mono pulse regime crystallizes in the anatase phase while that made in the multi-pulse regime crystallizes in the rutile form. As deposited films are sub-stoichiometric and after annealing the stoichiometries approach to that of TiO_2 . Film morphology reflects the effect of plasma re-excitation with the multi-pulsed laser, as more splashing and higher average height is observed; after annealing, surfaces are more homogenous although the film prepared with multi-pulsed laser keeps large surface particles that suggest they arise from the initial stages of deposition. The optical dispersion curves and the optical band gap behavior before and after

annealing, indicate the presence of TiO_x inclusions as well as a better compositional homogeneity in the film prepared in the multipulse regime. The results indicate that for the deposition with multi-pulse, the particles that impinged on the substrate have higher surface mobility than the corresponding particles for the single-pulse regime, confirming they come from plasma with higher energy than those from the single-pulse regime. Moreover, the results showed that it is possible to deposit black titania films (TiO_{2-x}) by PLD from TiO_2 , with the possibility to modulate the final phase, anatase or rutile, by changing the laser regime and annealing conditions. Future work is intended to explore the properties and applications either in photocatalysis and photovoltaics of such films.

Acknowledgments

LP is Invited Professor from San Petersburg Electrotechnical University. FCA is researcher on CONICET. This work was partially supported by Universidad Nacional de Quilmes under contract PUNQ1388/15 and PUNQ1406/15]. Research partially financed by SIP project MD-20161804/20170560. CGA is financed through the Catedras CONACYT grant number 1056.

ORCID iDs

F C Alvira  <https://orcid.org/0000-0002-8425-642X>

References

- [1] Smith H M and Turner A F 1965 Vacuum deposited thin films using a Ruby laser *Appl. Opt.* **4** 147–8
- [2] Gacek S and Wang X 2008 Dynamics evolution of shock waves in laser–material interaction *Appl. Phys. A* **94** 675–90
- [3] Meng L-J and dos Santos M P 1993 Investigations of titanium oxide films deposited by d.c. reactive magnetron sputtering in different sputtering pressures *Thin Solid Films* **226** 22–9
- [4] Eason R 2007 *Pulsed Laser Deposition of Thin Films* (Hoboken, NJ: Wiley)
- [5] Kushwaha A, Mohanta A and Thareja R K 2009 C_2 and CN dynamics and pulsed laser deposition of CNx films *J. Appl. Phys.* **105** 044902
- [6] Thareja R K and Mohanta A 2010 Gas suspended ZnO clusters and pulsed laser deposition of ZnO thin film *Phys. Status Solidi C* **7** 1413–6
- [7] György E, Mihailescu I N, Kompitsas M and Giannoudakos A 2002 Particulates-free Ta thin films obtained by pulsed laser deposition: the role of a second laser in the laser-induced plasma heating *Appl. Surf. Sci.* **195** 270–6
- [8] Galbács G, Jedlinszki N, Herrera K, Omenetto N, Smith B W and Winefordner J D 2010 A study of ablation, spatial, and temporal characteristics of laser-induced plasmas generated by multiple collinear pulses *Appl. Spectrosc.* **64** 161–72
- [9] Peñaloza-Mendoza Y and Ponce-Cabrera L 2015 Comparison on morphological and optical properties of TiO_2 thin films grown by single-pulse and multi-pulse laser ablation *Journal of Surface Engineered Materials and Advanced Technology* **5** 17–23
- [10] Rout S, Popovici N, Dalui S, Paramês M L, da Silva R C, Silvestre A J and Conde O 2013 Phase growth control in low temperature PLD Co: TiO_2 films by pressure *Current Applied Physics* **13** 670–6
- [11] Mamane H, Horovitz I, Lozzi L, Camillo D D and Avisar D 2014 The role of physical and operational parameters in photocatalysis by N-doped TiO_2 sol–gel thin films *Chem. Eng. J.* **257** 159–69
- [12] Yu Y-Y, Chien W-C, Ko Y-H and Chen S-H 2011 Preparation and characterization of P3HT:CuInSe₂: TiO_2 thin film for hybrid solar cell applications *Thin Solid Films* **520** 1503–10
- [13] Han K and Kim J H 2012 Fabrication of $\text{TiO}_2/\text{SiO}_2$ multilayer film structure by the sol–gel process with efficient thermal treatment methods *Appl. Surf. Sci.* **263** 69–72
- [14] Nguyen D C T, Cho K Y and Oh W C 2017 Synthesis of frost-like CuO combined graphene- TiO_2 by self-assembly method and its high photocatalytic performance *Appl. Surf. Sci.* **412** 252–61
- [15] Coto M, Divitini G, Dey A, Krishnamurthy S, Ullah N, Ducati C and Kumar R V 2017 Tuning the properties of a black TiO_2 –Ag visible light photocatalyst produced by a rapid one-pot chemical reduction *Materials Today Chemistry* **4** 142–9
- [16] Chierchia R, Menchini F, Serenelli L, Mangiapane P, Polichetti T and Tucci M 2016 Titanium oxide films deposited by e-beam evaporation as n-type electrode for solar cell applications *Physica Status Solidi (C) Current Topics in Solid State Physics* **13** 1002–5
- [17] Schönberger W, Bartsch H, Schippel S and Bachmann T 2016 Deposition of rutile TiO_2 films by pulsed and high power pulsed magnetron sputtering *Surf. Coat. Technol.* **293** 16–20
- [18] Sharma A K, Thareja R K, Willer U and Schade W 2003 Phase transformation in room temperature pulsed laser deposited TiO_2 thin films *Appl. Surf. Sci.* **206** 137–48
- [19] Alvira F C, Cabrera L P, Peñaloza Mendoza Y, Martinez Ricci M L and Videla F 2017 Pulsed laser deposition of PbTe under monopulse and multipulse regime *Opt. Lasers Eng.* **90** 284–90
- [20] Durand H A, Brimaud J H, Hellman O, Shibata H, Sakuragi S, Makita Y, Gesbert D and Meyrueis P 1995 Excimer laser sputtering deposition of TiO_2 optical coating for solar cells *Appl. Surf. Sci.* **86** 122–7
- [21] Mardare D, Tasca M, Delibas M and Rusu G I 2000 On the structural properties and optical transmittance of TiO_2 r.f. sputtered thin films *Appl. Surf. Sci.* **156** 200–6
- [22] Cronmeyer D C 1959 Infrared absorption of reduced rutile TiO_2 single crystals *Phys. Rev.* **113** 1222–6
- [23] De Giacomo A, Shakhmatov V A, Senesi G S and Orlando S 2001 Spectroscopic investigation of the technique of plasma assisted pulsed laser deposition of titanium dioxide *Spectrochimica Acta Part B: Atomic Spectroscopy* **56** 1459–72
- [24] Tauc J 1968 Optical properties and electronic structure of amorphous Ge and Si *Mater. Res. Bull.* **3** 37–46